

# INORGANIC CHEMISTRY

---

## FRONTIERS



CHINESE  
CHEMICAL  
SOCIETY



ROYAL SOCIETY  
OF CHEMISTRY




[rsc.li/frontiers-inorganic](https://rsc.li/frontiers-inorganic)

## REVIEW

[View Article Online](#)  
[View Journal](#) | [View Issue](#)

 Cite this: *Inorg. Chem. Front.*, 2020, **7**, 1319

# The synthesis and applications of chiral pyrrolidine functionalized metal–organic frameworks and covalent-organic frameworks

 Mi Zhou,<sup>a</sup> El-Sayed M. El-Sayed, <sup>a,b,c</sup> Zhanfeng Ju,<sup>a</sup> Wenjing Wang <sup>a</sup> and Daqiang Yuan <sup>\*a</sup>

Proline is a natural amino acid that can be considered as an excellent, efficient, and versatile organo-catalyst for various asymmetric reactions. The encapsulation of organocatalysts, such as proline and related derivatives, into a porous material, can not only construct a novel heterogeneous catalyst but also provide a platform to mimic and explore the catalytic processes in a biological system. In this regard, metal–organic frameworks (MOFs) and covalent-organic frameworks (COFs) show superiority because of their crystalline structure, rational designable and tunable framework. In this review, we mainly focus on chiral pyrrolidine functionalized MOFs and COFs; the synthetic strategies and related applications of these materials have been summarized systematically.

 Received 28th August 2019,  
 Accepted 3rd December 2019

DOI: 10.1039/c9qi01103j

[rsc.li/frontiers-inorganic](http://rsc.li/frontiers-inorganic)

## 1. Introduction

The twenty natural amino acids are essential substances for living systems; meanwhile, nineteen of them exist in nature with an L-configuration. The cheap and naturally available optically pure amino acids also play an indispensable role in chiral pools.<sup>1</sup> Among them, proline is distinctive because of its semi-rigid structure. Although proline has a simple structure and relatively small molecular size, the perfect combination of a secondary amine and a carboxylic acid in a semi-rigid molecule makes it an efficient and versatile organocatalyst for a series of asymmetric catalytic processes, including aldol reaction, Mannich reaction, Michael reaction, Diels–Alder reaction,  $\alpha$ -amination of aldehydes, and  $\alpha$ -alkylation of aldehydes.<sup>2,3</sup> And pyrrolidine–NH was proposed to be crucial for the activation of the aldehyde or ketone.

Due to their small molecular size, outstanding performance in asymmetric catalysis and facile functionalization, proline and related derivatives have been incorporated into porous silica<sup>4–6</sup> and traditional inorganic porous crystalline materials such as zeolite<sup>7,8</sup> to construct heterogeneous catalysts. However, these materials always display limited BET surface area; furthermore, the weak interaction of the host material

and the guest functional molecules always leads to undesired guest leaching. Covalently bonded polymer like resin<sup>9–12</sup> and porous organic polymers<sup>13–18</sup> also have been applied in heterogeneous catalysis, but the amorphous framework, irregular channel and widely distributed pore size inevitably lead to an uncontrollable catalytic environment.

Metal–organic frameworks (MOFs)<sup>19</sup> and covalent organic frameworks (COFs)<sup>20</sup> attract extensive attention for their potential magnetism,<sup>21,22</sup> adsorption,<sup>23,24</sup> luminescence,<sup>25,26</sup> and electrochemical applications.<sup>27–29</sup> Meanwhile, MOFs and COFs are advanced host platforms that can construct novel heterogeneous catalysts due to their long-range ordered structures, highly accessible surface areas, tunable and uniform channel sizes, and rational designable frameworks.<sup>30–36</sup> Among porous materials, MOFs and COFs possess advantages like: (a) a designable structure ensuring the feasibility of functionalization; (b) a crystalline framework providing a platform to install the functional fragments in a specific and ordered environment; and (c) diverse sites and various functionalization methods to fulfill efficient immobilization of various types of functional molecules.

From the point of application, the natural chiral and cheap proline with a relatively small molecular size is a perfect chiral source to insert into MOFs and COFs with channels from a few angstroms to a few nanometers. Moreover, the introduction of proline and related derivatives into well-defined frameworks such as MOFs and COFs may result in frameworks which are: (a) elegant materials for sensitive and accurate molecular recognition; (b) chiral heterogeneous catalysts with proline-like catalytic ability; (c) novel platforms to

<sup>a</sup>State Key Laboratory of Structural Chemistry, Fujian Institute of Research on the Structure of Matter, Chinese Academy of Sciences, Fuzhou 350002, China.

E-mail: ydq@fjirsm.ac.cn

<sup>b</sup>University of the Chinese Academy of Sciences, Beijing, China

<sup>c</sup>Chemical Refining Laboratory, Refining Department, Egyptian Petroleum Research Institute, Nasr City, Egypt

mimic and explore the functionality of the natural enzymes; and (d) hybrid frameworks for complex catalytic processes such as tandem catalysis and synergetic catalysis. It should be mentioned that this review is mainly focused on MOFs and COFs functionalized with proline or proline derivatives, while related research studies based on porous silica, zeolite, resin, and porous organic polymers are not included.

## 2. Chiral pyrrolidine-functionalized MOFs

In the past few decades, due to their porous, designable, crystalline, and organic-inorganic hybrid structures, MOFs have become an engaging research field. Due to the perfect combination of metal ions and organic linkers, MOFs are perceived as novel platforms to load active sites behaving as heterogeneous catalysts.<sup>37–41</sup> Evoked by the report of the pioneering work on homochiral MOFs by Kim *et al.*,<sup>42</sup> synthetic strategies such as chiral induction,<sup>43</sup> direct syntheses from privileged ligands,<sup>32,36,44</sup> coordinate postsynthetic modification,<sup>45,46</sup> covalent postsynthetic modification,<sup>47</sup> postsynthetic deprotection,<sup>48</sup> and linker exchange<sup>49</sup> have been established for desired chiral crystalline porous materials.<sup>50</sup>

In terms of functional molecular fragments, apart from achiral tectons such as salphen,<sup>51</sup> pyenH<sub>2</sub>,<sup>52</sup> and urea,<sup>53,54</sup> chiral molecular motifs such as salen,<sup>55–57</sup> binol,<sup>58–60</sup> binap,<sup>61,62</sup> spiro,<sup>63</sup> and proline also have been employed to construct MOFs as heterogeneous catalysts. In general, proline shows difficulty in assembling into 3-periodic frameworks due to its convergent molecular structure despite its versatile coordination behavior. The carboxylic group of proline can function as an efficient coordinate site with  $\mu_1$ -O,  $\mu_2$ -O, and even  $\mu_3$ -O coordinate modes. Simultaneously, N and O in each proline molecule are suitable for chelating metal ions synergistically (especially for soft Lewis acid metal ions) and form a stable five-membered ring due to the adjacent alignment of pyrrolidine-NH and the carboxylate group. However, the unoccupied secondary amine is fundamental for the catalytic potency of proline, and the occupied N site will lead to deactivation of proline (Fig. 1a and b).

To overcome the consequences generated by the convergent structure of proline, it is crucial to modify proline to qualify for the synthesis of MOFs. In the case of ligand design, the typical method to functionalize proline is based on the renovation of pyrrolidine-NH or the carboxylic acid (Scheme 1). Once again, there is no doubt that the functionalization of pyrroli-

dine-NH will block the catalytic site, while the modification of the carboxylic acid may furnish the pyrrolidine as a pendant fragment. Based on these ligands, except MOFs with a single proline site that have been published, complex systems such as MOFs with a combination of multiple active sites in one single framework for synergetic catalysis and tandem catalysis have also been established (Table 1). In general, these proline-based MOFs can be classified into four groups in terms of catalytic sites: (2.1) MOFs with blocked pyrrolidine-NH sites; (2.2) MOFs with single unoccupied pyrrolidine-NH; (2.3) pyrrolidine-functionalized MOFs with a tunable catalytic environment and (2.4) pyrrolidine-based MOFs with multi-catalytic sites.

### 2.1. MOFs with blocked pyrrolidine-NH sites

At the early stage of proline-based MOFs, commercially available proline was employed as a ligand to construct chiral frameworks directly. And it is common to produce a convergent structure or a 1D-chain structure with proline, rare studies on 2D or 3D extended structures have been reported.

In 2006, Su *et al.* employed proline as an organic chiral source for construction of a pair of chiral framework enantiomers with a high-charge Keggin-type polyoxometalate (POM). Proline binds to Cu(II) forming a 1D coordinated chain primarily, and then the chains were further imparted by [BW<sub>12</sub>O<sub>40</sub>]<sup>5-</sup> with Cu-O bonds to construct the 3-periodic framework. It should be mentioned that all the coordinate sites of proline take part in the self-assembly; so no accessible pyrrolidine-NH site exists in this framework.<sup>64</sup> This work reported the first pairs of proline-based homochiral open 3-periodic frameworks, and from then on reports about proline based frameworks started to spring up. In 2007, Rosseinsky *et al.* packed proline, 4,4'-bipyridyl (BPY), and Zn(II) or Cd(II) into two 2D coordination polymers. The 1D cationic chain constructed from proline and the metal ion was linked with BPY in the 2D plane; meanwhile, active pyrrolidine-NH was occupied by intra-layer hydrogen bonds and balanced anions.<sup>65</sup>

For building an extended 3-periodic chiral framework with proline efficiently, some multi-topic ligands by functionalizing pyrrolidine-NH have been designed and synthesized (Scheme 1). These ligands can aptly deliver chirality to MOFs but without proline-like catalytic activity. In 2006, Xiong *et al.* built a 3-periodic MOF based on the *in situ* synthesis of flexible **L1**. Due to the flexible nature of **L1**, the chiral **L1** based network crystallizes in a noncentrosymmetric space group without accessible pores; the crystal can be a potential candidate for second-order nonlinear materials and ferroelectric materials.<sup>66</sup>

In general, the presence of accessible pores and channels is crucial for applications such as adsorption,<sup>67,68</sup> molecular recognition,<sup>69</sup> and organic catalysis. Inspired by the excellent work of HKUST-1<sup>70</sup> on 1,3,5-benzenetricarboxylic acid (BTC) with a relatively small size, Zhang *et al.* designed the functional ligand **L2** by replacing one of the carboxylic groups of BTC with proline. After being self-assembled with Cu(II), two pairs of enantiomeric homochiral MOFs (**L-1/D-1** and **L-2/D-2**) were constructed with proline decorated cages, and the structural differ-

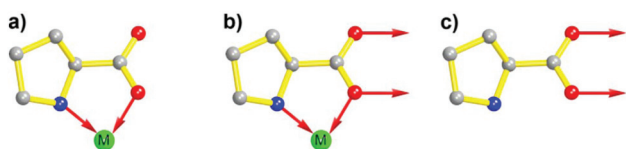


Fig. 1 The common coordinate mode for proline.





**Table 1** Heterogeneous catalysis based on chiral pyrrolidine functionalized MOFs

MOF	Active group	Catalytic reaction	Enantioselectivity	Ref.
L-1	Open Cu(II) site	Oxidative coupling	—	71
DUT-67-Pro	Pyrrolidine NH	Michael addition	25–38% ee	98
UiO-66-LP	Pyrrolidine NH	Aldol reaction	—	99
UiO-67-LP				
Zr-NDC-LP				
CMIL-1	Pyrrolidine NH	Aldol reaction	52–81% ee	102
CMIL-2	Open Cr(III) site			
CMIL-101	Amide group Open Cr(III) site	Reduction	34–37% ee	103
Zn-MOF1	Pyrrolidine NH	Aldol reaction	48–73% ee	104
Al-MIL-101-NH-Gly-Pro	Pyrrolidine NH	Aldol reaction	17–27% ee	106
IRMOF-Pro	Pyrrolidine NH	Aldol reaction	14–29% ee	107
DUT-32-NHPro	Pyrrolidine NH	Aldol reaction	—	109
L10/H <sub>2</sub> N-MIL-101(Al)	Pyrrolidine NH	Aldol reaction	20–29% ee	110
UiO-67-NHPro	Pyrrolidine NH	Aldol reaction	—	111
UiO-68-NHPro				
L <sub>Cu</sub> PRO	Pyrrolidine NH	Baylis–Hillman reaction	—	112
UHM-25-Pro	Pyrrolidine NH	Aldol reaction	40% ee	113
MTV-(CH <sub>3</sub> ) <sub>0.8</sub> (CH <sub>2</sub> NH–Pro–NH <sub>2</sub> ) <sub>0.2</sub>	Pyrrolidine NH	α-Chlorination of butyraldehyde	20% ee	117
MUF-77	Pyrrolidine NH	Aldol reaction	3.3–26.5% ee	124
MUF-77	Pyrrolidine NH	Aldol reaction	0.3–27.7% ee	125
Zn-PYI1	Pyrrolidine NH Triphenylamine	Photocatalytic α-alkylation of aliphatic aldehydes	78–92% ee	128
INP-1	Pyrrolidine NH Triphenylamine	Photocatalytic β-arylation of saturated aldehydes	28–55% ee	129
Ni-PYI1	Pyrrolidine NH [BW <sub>12</sub> O <sub>40</sub> ] <sup>5-</sup>	Tandem catalysis for epoxidation and hydrolysis	67–95% ee	131
ZnW-PYI1	Pyrrolidine NH [ZnW <sub>12</sub> O <sub>40</sub> ] <sup>6-</sup> Open Zn(II) site	Tandem catalysis for epoxidation and cycloaddition	55–96% ee	132
CuW-PYI1	Pyrrolidine NH [PW <sub>12</sub> O <sub>40</sub> ] <sup>3-</sup>	Tandem catalysis for aldol reaction and epoxidation	70.6–86.2% ee	133
CZJ-18(Cu)-Pro	Pyrrolidine NH Porphyrin–Cu(II)	Aldol reaction	29–88% ee	138
L16@3	Pyrrolidine NH Carboxylic acid	Aldol reaction	66–80% ee	140
MIL-101-PP1	Pyrrolidine NH Open Cr(III) site	Aldol reaction	87–96% ee	146

Although both enantiomers of these frameworks have been constructed in most of these references, only one of the enantiomers is displayed in this table for clarity.

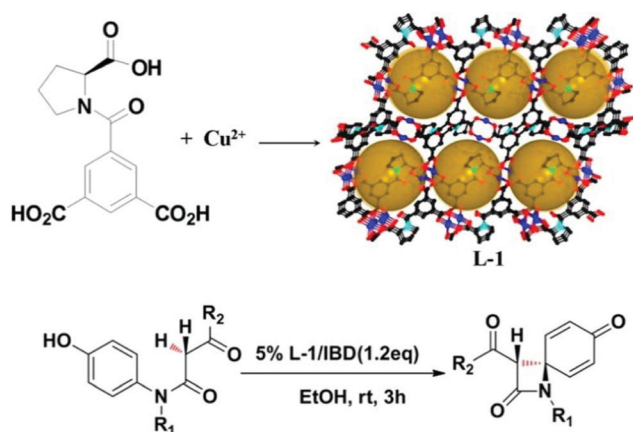


**Fig. 2** Schematic presentation of the construction of compound L-1 and the catalytic synthesis of β-lactam.

mixed-ligand strategy from semi-rigid **L2** and rigid 1,3,5-tri(1*H*-imidazol-1-yl)benzene (TIB) to react with Cd(II) for more porous MOFs. The afforded framework possesses two kinds of cage units and an *srs* topology with 49.2% porosity and 955.8 m<sup>2</sup> g<sup>-1</sup> BET surface area. Moreover, the chiral framework displays moderate enantioselective adsorption for methyl lactate (34.8% ee).<sup>75</sup>

In 2017, *via* extending the design strategy to 1,4-benzenedicarboxylic acid (BDC) and biphenyl-4,4'-dicarboxylic acid (BPDC), Wu *et al.* synthesized two flexible ligands **L3** and **L4** functionalized with two proline groups. The integration of bipyridyl ligands, metal ions, and **L3** or **L4** generated two pairs of ladderlike metal–organic layers with a nanoscale channel. Enantioselective adsorption experiments demonstrated that the metal–organic layer with a larger channel shows better enantioselectivity for a bulkier substrate—the ee value for the adsorbed substrate increases from 12.03% for 1-phenyl-1,2-ethanediol to 56.86% for hydrobenzoin and 67.44% for 1,1,2-triphenyl-1,2-ethane-diol.<sup>76</sup>

## 2.2. MOFs with single unoccupied pyrrolidine–NH

Due to the blockage of the pyrrolidine–NH group, the pyrrolidine fragment in the above-mentioned frameworks only functions as a linker to supply a chiral environment but without the catalytic capacity of proline. According to the proposed mechanism of proline catalysis, it is critical to maintain the pyrrolidine–NH group unoccupied to construct a framework with proline-like catalytic activity.

As is well-known, monocarboxylic acids are powerful regulators for highly crystallized MOFs with high-connected SBUs from rare-earth metals,<sup>77</sup> Ti(IV),<sup>78–80</sup> Hf(IV)<sup>81,82</sup> and Zr(IV).<sup>83,84</sup> As one kind of chiral monocarboxylic acid with an NH group in the *ortho*-position, proline not only provides versatile coordination modes for the efficient modulation of various SBUs,<sup>85</sup> but can also deliver chirality to MOFs from achiral components by chiral induction.<sup>86–88</sup> Based on the hard–soft–acid–base theory, it is reasonable to introduce proline into MOFs as a pendant ligand with a hard Lewis-acid metal. The carboxyl group of proline is expected to take part in the coordination while leaving pyrrolidine–NH unoccupied to construct a proline-based heterogeneous catalyst by defect engineering.<sup>89–93</sup>

The  $Zr_6O_4(OH)_4(CO_2)_n$  cluster is a famous SBU in constructing UIO-type MOFs, and it often acts as a 6-, 8- and 12-connected node.<sup>94</sup> Interestingly, the terminal coordinated  $HCO_2^-$  or  $CH_3CO_2^-$  for an 8-connected SBU can be replaced by other carboxylic ligands.<sup>95–97</sup> Employing the solvent-assisted linker incorporation strategy, Kaskel and Senkowska *et al.* introduced proline into 8-connected zirconium-based DUT-67 (Fig. 3). The terminal carboxyl groups in DUT-67 were replaced by proline completely with ligand exchange, which can be verified by  $^1H$  NMR of the digested sample (2,5-thiophenedicarboxylic acid/proline  $\approx 2:1$ ). Proline functionalized DUT-67-Pro shows activity to catalyze the asymmetric Michael reaction with a moderate ee value (38%). Besides, recycling and leaching experiments demonstrate that proline is firmly bonded to the framework with unoccupied pyrrolidine–NH.<sup>98</sup> To simplify the synthetic procedure, Van Der Voort *et al.* adopted a one-pot method to attach proline in UIO-66, UIO-67 and Zr-NDC with proline as an SBU modulator. Proline can be inserted into the defect of the zirconium cluster successfully. It was found that the decreased synthesis temperature resulted in higher ratio defects, while the stability of the framework decreased consequently. The resulting MOFs can not only catalyze the aldol

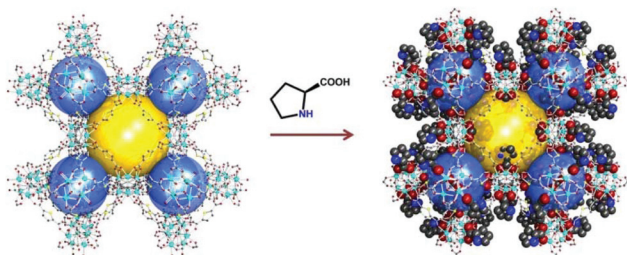


Fig. 3 Schematic presentation of defect engineered DUT-67 with L-proline.

reaction but also show interesting reversed diastereoselectivity to the homogeneous counterpart.<sup>99</sup>

As the carboxyl group is an efficient group for molecular decoration, ligands based on modifying the carboxyl group of proline have also been established. Zhang *et al.* designed L5 *via* substituting the carboxylic acid of proline with a tetrazole group. The combination of L5 and Zn(II) or Cd(II) afforded isostructural 2D chiral coordination polymers with pyrrolidine–NH taking part in the formation of a five-membered coordinate ring.<sup>100</sup> As pyrrolidine–NH is adjacent to the chelating carboxyl group, to alleviate the tendency of forming a coordinate ring, it is required to modify proline for an elongated ligand. Furthermore, this strategy may result in frameworks with the pyrrolidine protruding into the channel, which may alleviate the excessive hindrance of the channel and benefit the catalysis.

Amidation is a useful method to functionalize the carboxyl group, and several reports about monotopic pyrrolidine based ligands decorated with a pyridyl group have been published. MIL-101 has been extensively explored in the materials field for its robustness, high porosity and hierarchical porous structure, in which the labile terminal  $H_2O$  on the trichromium SBU can be substituted by an N-donor ligand.<sup>101</sup> Kim *et al.* reported the first case to construct chiral MIL-101 *via* coordinate postsynthetic modification (Fig. 4). Primarily, they designed and synthesized pyrrolidine functionalized L6 with a 3-pyridyl group and L7 with a 4-pyridyl group, and then L6 and L7 were attached to the SBUs of MIL-101 with a coordination bond to construct two MIL-101 based chiral frameworks. Both chiral frameworks exhibit better catalytic behavior than the corresponding homogeneous ligand toward asymmetric aldol reaction, and the superior enantioselectivity might have been derived from the multiple chiral inductions in the confined space of the heterogeneous catalyst. Interestingly, CMIL-101 functionalized with different ligands affords products with different ee values (76% for L6 *vs.* 58% for L7) although the two ligands only show different positions of the pyridyl group. This indicates that even a minor change of the catalyst may result in much different catalytic behavior. Moreover, the size-dependent experiment demonstrates the intrinsic pore catalysis, while the recycled experiment verifies that the strategy is powerful to load the homogeneous catalyst.<sup>102</sup>

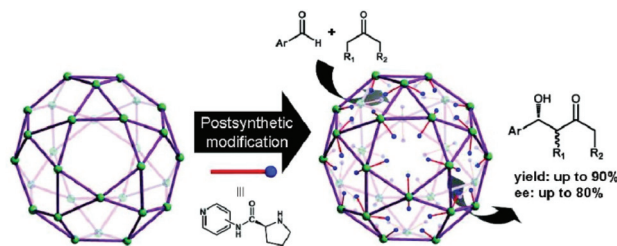


Fig. 4 Schematic depiction of coordinate postsynthetic modification of MIL-101 with proline-derived auxiliary ligands for heterogeneous catalysts.

Followed Kim's work, Zhang *et al.* found that both MIL-101 and the *N*-formyl pendant ligand **L8** are efficient catalysts for the reduction of ketimines. The integration of chiral **L8** and MIL-101 into a chiral heterogeneous catalyst was achieved through coordinate postsynthesis. The resulting material displays remarkable activity as a heterogeneous catalyst for the asymmetric reduction of ketimines (as high as 81% yield and 37% ee).<sup>103</sup>

Covalent postsynthetic modification is somewhat distinct from the strategy mentioned above *via* coordination bonds, and this method enables decoration on the organic linker of MOFs with stronger covalent bonds, which reminds us of the functional graft polymer. In 2012, Duan *et al.* synthesized two achiral MOFs with an ethynyl-decorated channel, and then the chiral 2-azidomethylpyrrolidine (**L9**) was anchored on the channel quantitatively *via* click reaction to construct the chiral framework. The resulting pyrrolidine functionalized hybrid material offers good catalytic activity and enantioselectivity toward the aldol reaction (as high as 76% yield and 73% ee).<sup>104</sup> With a different postsynthetic reaction, Canivet *et al.* adopted a solid-state peptide synthetic method to functionalize MOFs. In 2011, they modified In-MIL-68-NH<sub>2</sub> *via* creating peptide bonds in the framework. *N*-Fmoc proline was bound to the amine in the presence of a coupling agent and a weak base additive at room temperature. Relatively low yield was observed which may be related to the bulky Fmoc group and relatively small channel of MIL-68-NH<sub>2</sub>, though the protecting group can be removed quantitatively at room temperature in the system of piperidine/DMF.<sup>105</sup> To circumvent the low yield generated by the bulky Fmoc group, *N*-Boc amino acid was used for the modification of three amino-functionalized MOFs (Zr-Uio-66-NH<sub>2</sub>, In-MIL-68-NH<sub>2</sub>, and Al-MIL-101-NH<sub>2</sub>) with different porosity, topology, window size and pore size. Upon substituting the conventional heating with microwave irradiation, the reaction time can be shortened from 96 hours to 20 minutes dramatically, and Al-MIL-101-NH<sub>2</sub> can be modified with higher yield as a result of a bigger window and cavity in the framework. Furthermore, these pyrrolidine functionalized frameworks can catalyze the aldol reaction smoothly with a moderate ee value.<sup>106</sup>

Unlike postsynthetic modification that always has disadvantages such as pore blockage and decreased surface area and pore volume, the rational design and synthesis of targeted MOFs from a functional ligand are always fascinating as they endow MOFs with an explicit structure and uniformly distributed high-density functional sites. In 2011, Telfer *et al.* introduced the proline group into IRMOF-NHPro by designing a linear linker **L11** based on BPDC, and *N*-Boc protected **L11** was used to synthesize IRMOF-NHPro-Boc successfully. However, using only naked **L11** leads to unsuccessful attempts as a consequence of the interference of unoccupied pyrrolidine-NH in the self-assembly process. The introduction of the bulky Boc group not only ensures the successful synthesis of the targeted MOF but also restricts the framework interpenetration. Moreover, the Boc group will be decomposed into gaseous fragments after thermal treatment at 165 °C for 4 h (Fig. 5),

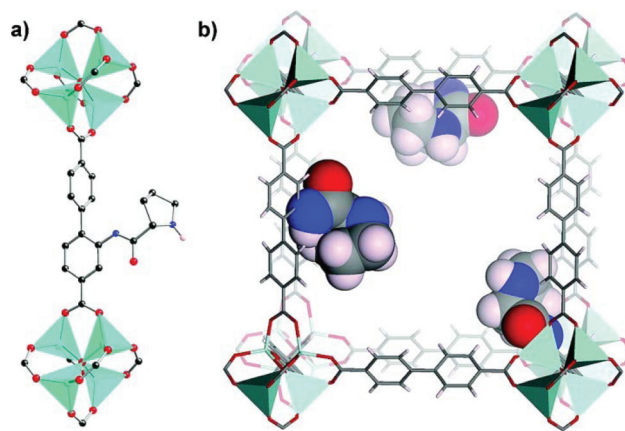


Fig. 5 The structure of IRMOF-Pro based on **L11**.

which will retain the unoccupied active sites in the framework. The resulting IRMOF-NHPro presents valuable activity and moderate enantioselectivity toward the aldol reaction (29% ee value).<sup>107</sup> This work evoked researchers to explore homochiral MOFs with rationally designed pyrrolidine functionalized linkers.

The functionality of MOFs with a hierarchical porous structure can be finely tuned with an elaborate choice of an organic linker and SBU, and the independent compartments with different environments in the single framework may be beneficial for diffusion and catalysis.<sup>108</sup> For this purpose, Kaskel *et al.* introduced **L11** into DUT-32. Obviously, thermal deprotection is inevitable for the full deprotection of *N*-Boc. Systematic research about the effect of thermal deprotection condition for DUT-32-NHProBoc on the ee value of the ligand was carried out; unfortunately, the results demonstrate that elevated temperature may lead to undesired racemization. With the temperature increasing to 140 °C, the ee value of the ligand decreased dramatically (Fig. 6), and this is unfavorable for the application of the material in asymmetric catalysis.<sup>109</sup>

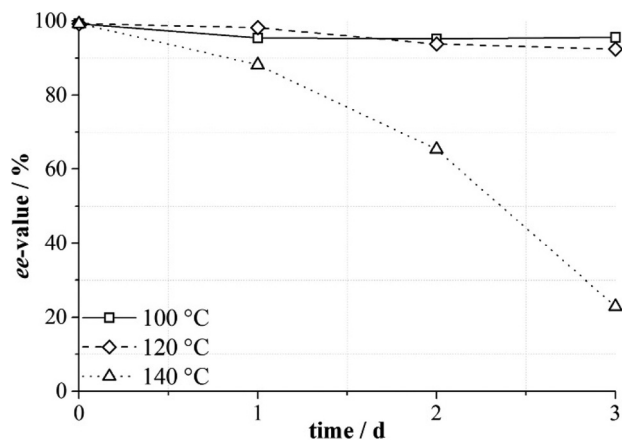


Fig. 6 Ee-value evolution of **L11** after heating in DMF at 100, 120, and 140 °C.



Compared to thermal treatment, acidic condition is a more effective method to deprotect the Boc group. The chirality of the organic ligands may be maintained in the presence of an acid under milder conditions. With this method, Janiak *et al.* introduced pyrrolidine functionalized **L10** into MIL-101(Al) *via* a mixed-ligand strategy, and the Boc group was deprotected simultaneously in the self-assembly process. In this way, the *in situ* deprotection of the Boc group without sacrificing the ee value of the ligand was attained. Although the framework affords products with a lower ee value (29% ee) compared to *L*-proline (66% ee), it is comparable to the homogeneous dimethyl ester of **L10** (21% ee). More importantly, the framework provides the product with reversed enantioselectivity (the framework affords an *S*-configuration product, while the homogeneous counterpart produces an *R*-configuration product), which can be attributed to the confinement effect of the framework.<sup>110</sup> In 2016, Kaskel *et al.* introduced **L11** and **L12** into isorecticular MOFs with different pore and channel sizes to investigate the influence of the cavity size on the catalysis (Fig. 7). They adopted a one-pot strategy to synthesize UIO-67-NHPro with **L11** and UIO-68-NHPro with **L12**, and the Boc group was removed spontaneously in an acidic synthetic system. The following heterogeneous catalysis illustrates that UIO-68-NHPro implies better performance than UIO-67-NHPro in catalyzing the aldol reaction due to the increased pore size and faster substrate diffusion rate (90% *vs.* 39% yield). Besides, these MOFs also feature unusual opposite diastereoselectivity compared with their homogeneous counterparts, which can be ascribed to the confinement effect of the catalytic site on the catalytic transition state.<sup>111</sup> In this manner, the innate configuration preference can be overridden through changing the energy barrier of the transition state when employing a particular MOF as a catalyst.<sup>99,111</sup>

In 2016, Bharadwaj and co-workers synthesized **L13** by replacing the benzoic acid of **L12** with an isophthalic acid moiety to construct a  $\text{Cu}_2(\text{CO}_2)_4$  based MOF. Rather than utiliz-

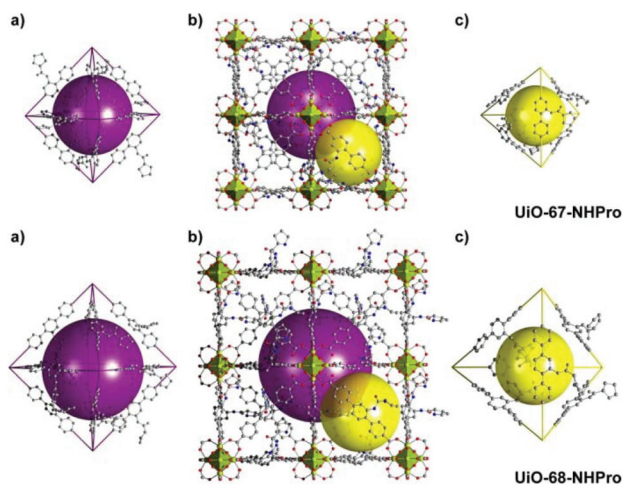


Fig. 7 Structures and cage units of UIO-67-NHPro (top) and UIO-68-NHPro (bottom).

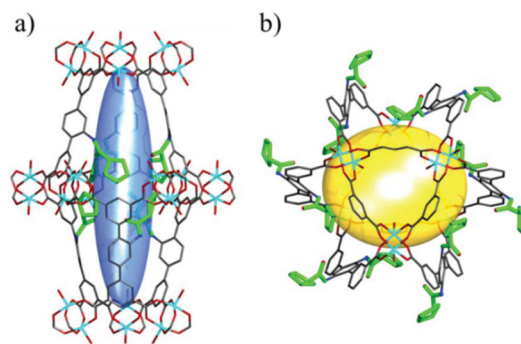


Fig. 8 Schematic presentation of (a) cage A and (b) cage B in  $\text{L}_{\text{Cu}}\text{PRO}$ ; the pyrrolidine groups are highlighted in bright green and hydrogen atoms are omitted for clarity.

ing the *N*-Boc protected ligand, a highly porous  $\text{Cu}_2(\text{CO}_2)_4$  based homochiral framework denoted as  $\text{L}_{\text{Cu}}\text{PRO}$  (63.1% porosity) with two kinds of cage units can be fabricated from unprotected **L13** directly. The Lewis-basic proline groups all point to the center of cage A to form a catalytic pocket (Fig. 8a); meanwhile, the substrate and product can diffuse in the framework *via* cage B freely (Fig. 8b). Experiments revealed that this MOF is a considerable catalyst for the Baylis–Hillman reaction (as high as 75% yield).<sup>112</sup> Fröba *et al.* introduced a series of chiral amino acids into a semi-rigid diisophthalic ligand to decorate the  $\alpha,\alpha$ -diaryl amino alcohol-based tetracarboxylic ligand **L14** (Fig. 9). A series of isostructural MOFs denoted as UHM-25 crystallized in a cubic space group with a rare *ucp* topology can be obtained either with *N*-Boc protected or unprotected ligands. Surprisingly, a much lower BET value can be observed for the nonprotected MOFs than for the *N*-Boc protected MOFs (371.5  $\text{m}^2 \text{g}^{-1}$  *vs.* 1922  $\text{m}^2 \text{g}^{-1}$  for UHM-25-Val to UHM-25-Val-Boc), and it is possibly due to the blockage of solvent molecules bonded with the naked amine group or partial collapse of the framework upon activation. UHM-25-Pro also can catalyze the aldol reaction with a moderate ee value (40%).<sup>113</sup> Based on the above results, it should be concluded that the *N*-Boc protecting group is not necessary for the synthesis of MOFs with a  $\text{Cu}_2(\text{CO}_2)_4$  SBU but is crucial for the construction of MOFs with a  $\text{Zn}_4\text{O}(\text{CO}_2)_6$  SBU.

### 2.3. Pyrrolidine-functionalized MOFs with a tunable catalytic environment

The complexity of an enzyme reflects that beside the active site, the surrounding environment is also crucial for the elegant molecular recognition and excellent catalytic efficiency. MOFs with the same backbone but different channel environments no doubt can provide an ideal platform to examine the effects of the surrounding environment on the catalytic activity.

IRMOF-74 is a class of robust and highly porous MOFs with good functional-group tolerance and may be competent in constructing a complex environment with multi-step postsynthetic modifications.<sup>114</sup> The derived IRMOF-74-III with an elongated ligand containing an augmented mesoporous hexag-





Fig. 9 Overview of the different types of linkers used in the UHM-25 MOFs.

onal channel (about 25 Å) has been proven to be a perfect candidate for post-functionalization.<sup>115,116</sup> In 2016, Yaghi *et al.* successfully realized the sequential installation of tripeptides in IRMOF-74-III *via* seven steps of tandem reactions with an

overall yield of 57% and an average yield of 93% for each step (Fig. 10); meanwhile, the crystallinity and permanent porosity of the framework can be maintained after multiple microwave-assisted deprotection and amino acid coupling reactions, which demonstrates that this framework is tolerant to these operations. Moreover, it was detected that aliphatic amine ( $\text{CH}_2\text{NHBoc}$ ) functionalized IRMOF-74-III exhibits higher reactivity than the framework decorated with an aromatic amine under the identical conditions ( $\sim 97\%$  vs.  $\sim 0\%$  yield for anchoring Ala). A further test shows that proline decorated IRMOF-74-III acts as an active catalyst for the  $\alpha$ -chlorination of butyraldehyde and affords higher enantioselectivity than its homogeneous counterpart (20% vs. 2% ee).<sup>117</sup> This work not only provides an efficient route to construct a complex environment in the mesoporous MOF but also entitles MOFs to act as a container to synthesize complex compounds with multi-step reactions; furthermore, the channel environment can be finely designed and modified *via* choosing and combining the substrate appropriately.

Rather than the randomly distributed variable components in post-synthesized MOFs and MTV-MOFs,<sup>118</sup> each variant in multicomponent MOFs such as MOF-205, MOF-210,<sup>119</sup> UMCM-1-5,<sup>120,121</sup> PCN-700-703,<sup>95</sup> LIFM-28,<sup>122</sup> and MUF-7x<sup>123</sup> is orderly distributed in the frameworks. So the catalytic environment of multicomponent MOFs can be finely regulated *via* elaborately changing the modulator ligands. In 2017, Telfer *et al.* engineered proline functionalized L10 and L11 into multicomponent MUF-77 with three types of ligands located at specific sites, and the spatial environment of the catalytic pocket can be programmed precisely by tuning the side arm of the other two linkers for the unique structure of MUF-77 consequently; in this manner, the catalytic activity can be modulated efficiently (Fig. 11). As expected, asymmetric aldol reaction indicates that the observed rate constant and enantioselectivity are related to the modulator ligand, with the increasing of the steric-hindrance from the side arms, the rate constant decreases significantly; furthermore, even the con-

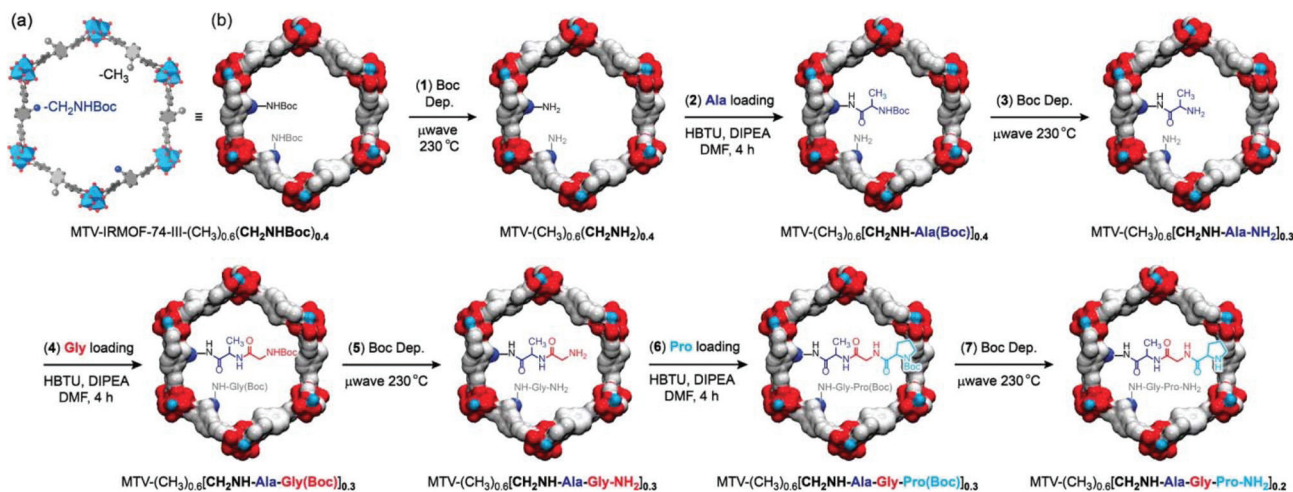


Fig. 10 Seven post-synthetic reactions to achieve enzyme-like complexity in the pores of MTV-IRMOF-74-III-( $\text{CH}_3$ )<sub>0.6</sub>( $\text{CH}_2\text{NHBoc}$ )<sub>0.4</sub>.



**Fig. 11** Schematic depiction of a pore in MUF-77 equipped with a site for catalysis and modulator groups that are positioned to modulate the environment of the reaction.

figuration of the preferred enantiomer can be reversed with the careful control of the spatial environment.<sup>124,125</sup>

#### 2.4. Pyrrolidine-functionalized MOFs with multi-catalytic sites

The hybrid and crystalline nature of MOFs provides an opportunity to distribute two or more catalytic sites in one single framework uniformly, and the resulting adduct may act as a unique catalyst for synergetic catalysis and tandem catalysis.<sup>126,127</sup> Upon encapsulation of chiral pendant ligand **L15** and photoactive 4,4',4''-tricarboxyltriphenylamine (TCA) in one framework, Duan *et al.* reported a MOF with excellent asymmetric photocatalytic activity (Fig. 12). The  $\alpha$ -alkylation of aliphatic aldehydes can be catalyzed by the hybrid framework smoothly (85% yield) with excellent enantioselectivity (92% ee). However, only negligible amounts of products can be harvested when the experiments are carried out in the dark or with a bulkier aldehyde, which indicates the photocatalytic and heterogeneous nature of this reaction. The physical mixture of an achiral TCA-based MOF and **L15** only leads to a moderate ee value (<24%), which expresses the superiority of the strategy in combining a photocatalyst and an asymmetric catalyst in one framework for synergetic catalysis. They proposed that the photoinduced electron can be reduced by the excited TCA ligand to form a radical anion, and then the Br-C bond in diethyl 2-bromomalonate was cleaved by the radical anion to afford an electrophilic radical and a bromide anion; finally, the electrophilic radical combines with the proline acti-

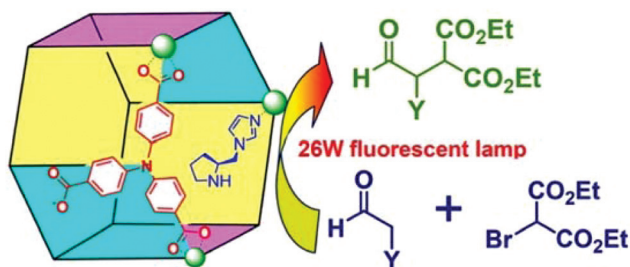


**Fig. 12** Schematic presentation of integrating photocatalytic TCA and **L15** in one framework for  $\alpha$ -alkylation of aliphatic aldehydes.

vated enamine to furnish the photocatalytic product.<sup>128</sup> Following this work, they harvested another 2-fold interpenetrated photocatalytic chiral MOF with a mono-zinc node, TCA and **L15** by modifying the synthetic conditions. Further tests explicate that not only the photocatalytic  $\beta$ -arylation of saturated ketones can be realized by the MOF smoothly (87% yield) with a moderate ee value (55%), but also the encapsulation and activation of the aldehyde by hydrogen bonds with the pyrrolidine can be captured and demonstrated by single-crystal XRD and spectral measurements systematically. This case not only shows that a novel catalyst can be constructed with MOFs, but also indicates that MOFs can provide more information about the activation process and the transition state.<sup>129</sup>

Polyoxometalate is a class of interesting chemicals with prominent redox activity.<sup>130</sup> Following a similar strategy, a chiral polyoxometalate-based Ni-PYI was synthesized with the integration of 4,4'-bipyridine, oxidative  $[\text{BW}_{12}\text{O}_{40}]^{5-}$ , chiral ligand **L15** and Ni(II), and the Boc group can be removed simultaneously under the acidic conditions. In this way, the encapsulation of the polyoxometalate and pyrrolidine ligand into a 3-periodic chiral oxidative framework was realized. The amphipathic framework proves to be an excellent container and catalyst for asymmetric one-pot tandem catalysis reaction of epoxidation and hydrolysis (Fig. 13). The framework yields dihydroxylated products from a mixture of a hydrophobic aryl olefin and a hydrophilic aqueous oxidant with 79% yield and an ee value as high as 95%. Meanwhile, the hydrolysis of the racemic 2-phenyloxirane only affords racemic products, indicating that the epoxidation reaction of the aryl olefin is the enantioselectivity-determining step. A size-dependent experiment and filtration experiment confirm the heterogeneous and pore-catalysis nature of the reaction.<sup>131</sup> Then,  $\text{NH}_2$ -bipyridine,  $[\text{ZnW}_{12}\text{O}_{40}]^{6-}$ , **L15** and Zn(II) were assembled into another chiral framework with an open Zn(II) site, a Brønsted basic site, and a redox-active polyoxometalate. The initial test shows that the framework can catalyze the epoxidation of the aryl olefin enantioselectively (94% yield and 93% ee). As the open Zn(II) site is an efficient catalyst for  $\text{CO}_2$  cyclic addition,

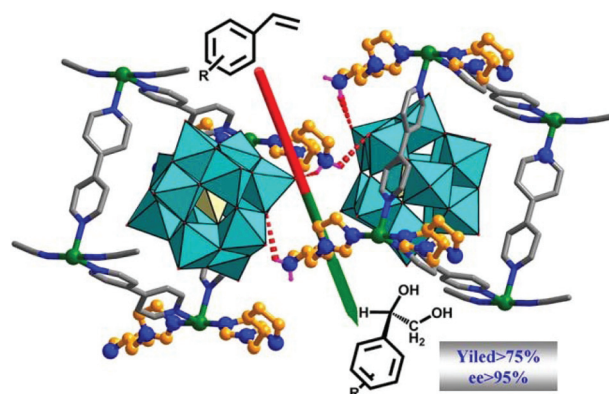


**Fig. 13** Schematic presentation of ZnW-PYI consisting of POM and **L15** for tandem catalysis.

the *in situ* formed epoxy compounds can be converted into high-value chiral cyclic carbonates with as high as 99% yield and 96% ee in the presence of CO<sub>2</sub>, ZnW-PYI and a cocatalyst. In contrast, a product with only a trace ee value was harvested when a racemic styrene oxide was employed as the starting material, which once again emphasizes that the enantioselectivity comes from the epoxidation rather than from the CO<sub>2</sub> cycloaddition reaction.<sup>132</sup> Furthermore, Li and Han *et al.* assembled oxidative PW<sub>12</sub>O<sub>40</sub><sup>3-</sup>, chiral **L15** and Lewis acid Cu(II) into a chiral polyoxometalate framework with a Kagomé structure. It was ascertained that the framework could catalyze the asymmetric cascade reaction of the aldol and epoxidation reaction. The dehydrated substance of the aldol reaction followed by epoxidation supplied the product with as high as 72.5% yield and 86.2% ee value.<sup>133</sup>

Metalloporphyrin is another kind of star molecule, and the metalloporphyrinic MOFs exhibit impressive catalytic performance in oxidation<sup>134–136</sup> and CO<sub>2</sub> fixation.<sup>137</sup> In 2019, Wu *et al.* constructed a 3-periodic MOF with the reaction of a metalloporphyrinic ligand and Y(III). Interestingly, the Y<sub>3</sub> SBU binds to eight carboxylates with another terminal acetate as a balanced anion due to the bulky size and steric hindrance of the metalloporphyrinic ligand. Additionally, the balanced terminal acetate can be substituted by monocarboxylic ligands such as proline and 4-sulfobenzoate; so the pendant ligand and the central metal of porphyrin can be tuned systematically. With the systematic modification of the structure, the resulting framework proves to be a versatile catalyst for the epoxidation of olefins, aerobic oxidation of alcohols, and aldol reaction. The proline functionalized framework can catalyze asymmetric aldol reaction with excellent activity and ee values, and this MOF shows higher diastereoselectivity than the homogeneous L-proline.<sup>138</sup>

Apart from the organic linker and inorganic node of MOFs, the cavity of MOFs can also be exploited to incorporate functional guests. From the proposed catalytic mechanism of proline based aldol reaction, a Brønsted acid is also critical for high efficiency.<sup>139</sup> For realizing the priority of the adduct toward the homogeneous competitor, a reliable strategy is to impart those functional fragments in one framework. In 2014, Cui *et al.* synthesized a homochiral MOF with free carboxylic acids aligned along the nano-sized channel, and the (*S*)-2-(dimethylaminomethyl)-pyrrolidine (**L16**) was then accommodated in the channel *via* acid–base interactions (Fig. 14). The adduct presents comparable activity and superior enantioselectivity than its homogeneous counterpart in catalyzing aldol reactions, which might have been derived from the syner-

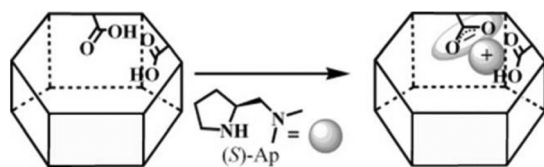


Fig. 14 Schematic depiction of encapsulating **L16** in the MOF with the free carboxylic acid; the frame presents the host MOF.

gistic effect of the free carboxylic acid and the introduced pyrrolidine derivative in the confined chiral space.<sup>140</sup>

Linear organic polymers are a class of useful functional materials; however, this kind of material always possesses a relatively low BET and an irregular channel. The hybridization of functional polymers and MOFs *in situ* not only can increase the accessible polymer surface for the substrate but also endow MOFs with unique functionality.<sup>141–145</sup> Liu and Dong *et al.* realized the *in situ* mixed polymerizations of vinyl derivatives (**L17**) to heterogenize a pyrrolidine-functionalized linear polymer into the pore of MIL-101 for heterogeneous chiral catalysis. The crystallinity of MIL-101 was maintained although the hybrid material showed a decreased BET surface area due to the inclusion of the polymer. Furthermore, the hybrid material proved to be an excellent heterogeneous catalyst for asymmetric aldol reaction due to the coexistence of a chiral pyrrolidine fragment and an unoccupied Cr(III) Lewis acid site (as high as 89% yield and 96% ee value).<sup>146</sup>

### 3. Pyrrolidine-functionalized COFs

COFs are a class of porous covalently bonded crystalline frameworks, and compared to the coordinate bonds of MOFs, the stronger linkage endows the framework with higher stability toward harsher conditions in the catalytic process. Although chiral catalytic fragments such as salen,<sup>147–150</sup> binol,<sup>151</sup> tartaric acid derivatives,<sup>152–154</sup> *S*-(+)-2-methylpiperazine<sup>155</sup> and pyrrolidine<sup>156–160</sup> have been inserted into COFs, chiral COFs are still relatively rare.<sup>161</sup> In general, the pyrrolidine moiety is incorporated into the COFs *via* covalent postsynthetic modification or direct synthesis with an *N*-Boc protecting group to avoid the undesired side reaction.

#### 3.1. Covalent postsynthetic modification

Jiang *et al.* reported the first chiral COF *via* postsynthetic modification in 2014. Firstly, they synthesized an achiral COF with alkynyl groups decorated along the square channel. Then, a click reaction was carried out with **L9** to install the chiral pyrrolidine on the wall of the COF with the crystallinity of the framework being maintained (Fig. 15). Catalytic experiments illustrate that this pyrrolidine functionalized chiral COF can catalyze the Michael reaction with good yield and moderate enantioselectivity in a 1:1 mixed solution of H<sub>2</sub>O/EtOH. Besides, the reaction rate is correlated with the ratio of the postsynthesized pyrrolidine. Maybe as a result of the blocked channel and delayed diffusion rate of the substrate, the reaction rate tends to decrease with an increased pyrrolidine loading ratio.<sup>156</sup> Furthermore, another mesoporous chiral COF with honeycomb pores was constructed using a similar strategy, and the obtained material shows outstanding catalytic activity with excellent diastereoselectivity and enantioselectivity in the H<sub>2</sub>O system.<sup>157</sup> These pioneering studies reported the novel strategy to construct chiral COFs, and prominent asymmetric catalysis in a green solvent was realized based on these COFs.



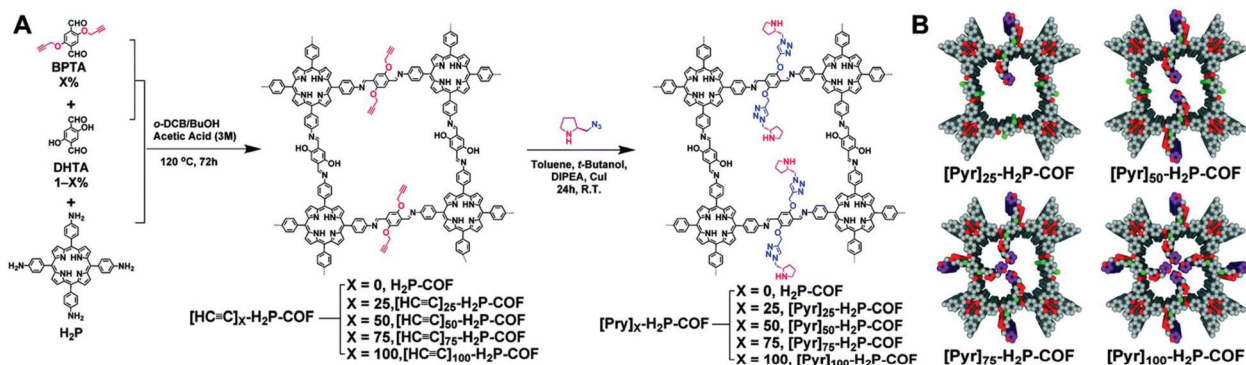


Fig. 15 Schematic presentation of the postsynthetic strategy to construct a proline based chiral COF.

### 3.2. Direct synthesis

For avoiding the harmful effects of postsynthetic modification such as reduced accessible surface area, cavity blockage, and randomly distributed catalytic sites, it is reasonable to design and construct chiral COFs from chiral monomers *via* direct synthesis. In this way, *N*-Boc protected pyrrolidine has been installed on rigid ditopic and tritopic monomers as a side arm (Scheme 2).

In 2016, Wang *et al.* designed and synthesized a chiral diamine ligand **L18** by attaching a pyrrolidine moiety to an achiral linear monomer. Two chiral COFs denoted as LZU-72 and LZU-76 were constructed from the chiral monomer with 1,3,5-triformylbenzene or triformylphloroglucinol, respectively (Fig. 16). Due to the assistance of intramolecular hydrogen bonds,<sup>162</sup> LZU-76 shows higher stability than LZU-72. Meanwhile, LZU-76 exhibits excellent activity and enantioselectivity for aldol reactions (as high as 84% yield and 88% ee).<sup>158</sup>

In 2017, Cui *et al.* anchored a series of chiral unit-like pyrrolidine (**L19**) compounds and a Macmillan catalyst to triamine monomers. 2D MTV-COFs were constructed from these monomers with linear dimethoxyterephthalaldehyde as the chiral moiety protruding into the hexagonal channel. The COFs with different chiral molecular fragments exhibit excellent activities to catalyze a batch of asymmetric reactions such as  $\alpha$ -aminoxylation of aldehydes, aldol reaction, and Diels–Alder reaction.<sup>159</sup> Recently, they extended this strategy for the synthesis of chiral trialdehyde monomers (**L20**), and 2D chiral COFs with a chiral moiety were harvested consequently when

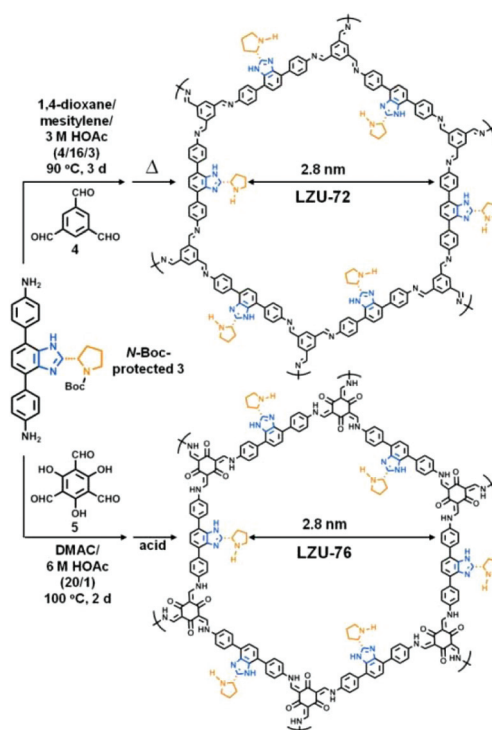
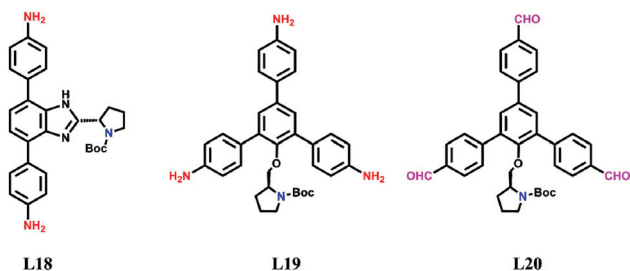


Fig. 16 Schematic presentation of the synthesis of LZU-72 and LZU-76.

these monomers reacted with the triamine monomer. The pyrrolidine functionalized COFs are perceived as outstanding catalysts for the asymmetric Michael addition and Steglich rearrangement reaction.<sup>160</sup>



Scheme 2 Structure of a proline functionalized monomer for COFs.

## 4. Summary and outlook

Until now, proline and related derivatives have been employed to synthesize chiral MOFs directly; furthermore, the strategies such as ligand design and postsynthetic modification have also been adopted to construct chiral MOFs and COFs with active unoccupied pyrrolidine–NH. Asymmetric catalytic processes, including characteristic proline catalysis, synergistic cat-

alysis, and tandem catalysis, with the obtained frameworks as heterogeneous catalysts have also been established.

It can be envisioned that except the recyclability for the heterogeneous catalysts, porous crystalline frameworks may participate in some unique applications. Firstly, these frameworks can be employed to conduct substrate or product size-selective catalysis. Despite catalytic site like pyrrolidine in the crystalline framework maybe not as active as the homogeneous counterpart for hampered diffusion rates and the tendency of coordination saturation<sup>163</sup> for active sites in the self-assembly process. However, the confinement effect of MOFs and COFs derived from the windows, pores, and walls of the framework may mitigate the side reaction and even override the innate molecular preference through changing the energy barrier of the transition state for specific molecules. Secondly, the porous frameworks can be utilized to explore the generic activation mode of the catalytic mechanism and determine the active transition-state species with MOFs. Due to the crystalline character, especially the single-crystal nature of most MOFs, the extra lattice energy and steric hindrance make it possible to develop active MOFs as crystalline sponge<sup>164,165</sup> to stabilize the transition-state species, and this can be measured by single-crystal X-ray diffraction directly. Finally, the scope of heterogeneous catalytic reactions with crystalline frameworks as catalysts may be extended with COFs. Due to the relatively fragile nature of the coordination bonds in MOFs, most of them are unstable to acids, bases, and even moisture. For the COFs with a stronger linkage, it may provide an opportunity to conduct the heterogeneous reaction under harsher conditions such as in aqueous, acidic, and basic media. This undoubtedly will broaden the range of the catalytic reaction with COFs as heterogeneous catalysts.

## Conflicts of interest

There are no conflicts to declare.

## Acknowledgements

This work was supported by the Strategic Priority Research Program of the Chinese Academy of Sciences (XDB20000000), the Key Research Program of Frontier Sciences, Chinese Academy of Sciences (QYZDB-SSW-SLH019), and the National Natural Science Foundation of China (21905281 and 21771177).

## Notes and references

- H. U. Blaser, *Chem. Rev.*, 1992, **92**, 935–952.
- D. W. MacMillan, *Nature*, 2008, **455**, 304–308.
- B. List, *Acc. Chem. Res.*, 2004, **37**, 548–557.
- C. Yu and J. He, *Chem. Commun.*, 2012, **48**, 4933–4940.
- P. Van der Voort, D. Esquivel, E. De Canck, F. Goethals, I. Van Driessche and F. J. Romero-Salguero, *Chem. Soc. Rev.*, 2013, **42**, 3913–3955.
- S. Lacasta, V. C. Sebastián, C. Casado, A. L. Mayoral, P. Romero, A. N. Larrea, E. Vispe, P. López-Ram-de-Viu, S. Uriel and J. N. Coronas, *Chem. Mater.*, 2011, **23**, 1280–1287.
- B. M. Weckhuysen, A. A. Verberckmoes, L. Fu and R. A. Schoonheydt, *J. Phys. Chem.*, 1996, **100**, 9456–9461.
- K. Arya, U. C. Rajesh and D. S. Rawat, *Green Chem.*, 2012, **14**, 3344–3351.
- M. Benaglia, A. Puglisi and F. Cozzi, *Chem. Rev.*, 2003, **103**, 3401–3429.
- K. Cho, J. Yoo, H.-W. Noh, S. M. Lee, H. J. Kim, Y.-J. Ko, H.-Y. Jang and S. U. Son, *J. Mater. Chem. A*, 2017, **5**, 8922–8926.
- S. Luo, J. Li, L. Zhang, H. Xu and J. P. Cheng, *Chem. – Eur. J.*, 2008, **14**, 1273–1281.
- G. Wulff, *Chem. Rev.*, 2002, **102**, 1–28.
- J. Schmidt, D. S. Kundu, S. Blechert and A. Thomas, *Chem. Commun.*, 2014, **50**, 3347–3349.
- J. Dong, Y. Liu and Y. Cui, *Chem. Commun.*, 2014, **50**, 14949–14952.
- Q. Sun, Z. Dai, X. Meng and F.-S. Xiao, *Chem. Soc. Rev.*, 2015, **44**, 6018–6034.
- D. Reinhard, W.-S. Zhang, Y. Vaynzof, F. Rominger, R. R. Schröder and M. Mastalerz, *Chem. Mater.*, 2018, **30**, 2781–2790.
- P. Chen, J.-S. Sun, L. Zhang, W.-Y. Ma, F. Sun and G. Zhu, *Sci. China Mater.*, 2018, **62**, 194–202.
- W. J. Wang, M. Zhou and D. Q. Yuan, *J. Mater. Chem. A*, 2017, **5**, 1334–1347.
- O. M. Yaghi, G. Li and H. Li, *Nature*, 1995, **378**, 703–706.
- A. P. Cote, A. I. Benin, N. W. Ockwig, M. O’Keeffe, A. J. Matzger and O. M. Yaghi, *Science*, 2005, **310**, 1166–1170.
- K. Liu, X. Zhang, X. Meng, W. Shi, P. Cheng and A. K. Powell, *Chem. Soc. Rev.*, 2016, **45**, 2423–2439.
- F. Ma, J. Xiong, Y.-S. Meng, J. Yang, H.-L. Sun and S. Gao, *Inorg. Chem. Front.*, 2018, **5**, 2875–2884.
- N. C. Burtch and K. S. Walton, *Acc. Chem. Res.*, 2015, **48**, 2850–2857.
- Z. W. Wang, M. Chen, C. S. Liu, X. Wang, H. Zhao and M. Du, *Chem. – Eur. J.*, 2015, **21**, 17215–17219.
- S. A. Diamantis, A. Margariti, A. D. Pournara, G. S. Papaefstathiou, M. J. Manos and T. Lazarides, *Inorg. Chem. Front.*, 2018, **5**, 1493–1511.
- Y. Cui, B. Li, H. He, W. Zhou, B. Chen and G. Qian, *Acc. Chem. Res.*, 2016, **49**, 483–493.
- H. Liu, H. Li, F. Cheng, W. Shi, J. Chen and P. Cheng, *Inorg. Chem.*, 2018, **57**, 10640–10648.
- R. Zhao, Z. Liang, S. Gao, C. Yang, B. Zhu, J. Zhao, C. Qu, R. Zou and Q. Xu, *Angew. Chem., Int. Ed.*, 2019, **58**, 1975–1979.
- J. Lv, Y. X. Tan, J. Xie, R. Yang, M. Yu, S. Sun, M. D. Li, D. Yuan and Y. Wang, *Angew. Chem., Int. Ed.*, 2018, **57**, 12716–12720.

- 30 J. Lee, O. K. Farha, J. Roberts, K. A. Scheidt, S. T. Nguyen and J. T. Hupp, *Chem. Soc. Rev.*, 2009, **38**, 1450–1459.
- 31 L. Ma, C. Abney and W. Lin, *Chem. Soc. Rev.*, 2009, **38**, 1248–1256.
- 32 M. Yoon, R. Srirambalaji and K. Kim, *Chem. Rev.*, 2012, **112**, 1196–1231.
- 33 A. H. Chughtai, N. Ahmad, H. A. Younus, A. Laypkov and F. Verpoort, *Chem. Soc. Rev.*, 2015, **44**, 6804–6849.
- 34 G. Kumar and S. K. Das, *Inorg. Chem. Front.*, 2017, **4**, 202–233.
- 35 S. M. J. Rogge, A. Bavykina, J. Hajek, H. Garcia, A. I. Olivos-Suarez, A. Sepúlveda-Escribano, A. Vimont, G. Clet, P. Bazin, F. Kapteijn, M. Daturi, E. V. Ramos-Fernandez, F. X. Llabrés i Xamena, V. Van Speybroeck and J. Gascon, *Chem. Soc. Rev.*, 2017, **46**, 3134–3184.
- 36 G. Yuan, H. Jiang, L. Zhang, Y. Liu and Y. Cui, *Coord. Chem. Rev.*, 2019, **378**, 483–499.
- 37 H. He, Y. Q. Xue, S. Q. Wang, Q. Q. Zhu, J. Chen, C. P. Li and M. Du, *Inorg. Chem.*, 2018, **57**, 15062–15068.
- 38 Y. X. Tan, X. Yang, B. B. Li and D. Yuan, *Chem. Commun.*, 2016, **52**, 13671–13674.
- 39 L. Liang, C. Liu, F. Jiang, Q. Chen, L. Zhang, H. Xue, H. L. Jiang, J. Qian, D. Yuan and M. Hong, *Nat. Commun.*, 2017, **8**, 1233.
- 40 J. Liu, L. Chen, H. Cui, J. Zhang, L. Zhang and C. Y. Su, *Chem. Soc. Rev.*, 2014, **43**, 6011–6061.
- 41 L. Jiao, Y. Wang, H. L. Jiang and Q. Xu, *Adv. Mater.*, 2018, **30**, e1703663.
- 42 J. S. Seo, D. Whang, H. Lee, S. I. Jun, J. Oh, Y. J. Jeon and K. Kim, *Nature*, 2000, **404**, 982–986.
- 43 R. E. Morris and X. Bu, *Nat. Chem.*, 2010, **2**, 353–361.
- 44 T. Drake, P. Ji and W. Lin, *Acc. Chem. Res.*, 2018, **51**, 2129–2138.
- 45 Z. Wang and S. M. Cohen, *Chem. Soc. Rev.*, 2009, **38**, 1315–1329.
- 46 J. D. Martell, L. B. Porter-Zasada, A. C. Forse, R. L. Siegelman, M. I. Gonzalez, J. Oktawiec, T. Runcevski, J. Xu, M. Srebro-Hooper, P. J. Milner, K. A. Colwell, J. Autschbach, J. A. Reimer and J. R. Long, *J. Am. Chem. Soc.*, 2017, **139**, 16000–16012.
- 47 Z. Wang and S. M. Cohen, *J. Am. Chem. Soc.*, 2007, **129**, 12368–12369.
- 48 S. M. Cohen, *Chem. Rev.*, 2012, **112**, 970–1000.
- 49 C. Tan, X. Han, Z. Li, Y. Liu and Y. Cui, *J. Am. Chem. Soc.*, 2018, **140**, 16229–16236.
- 50 Z. Han, W. Shi and P. Cheng, *Chin. Chem. Lett.*, 2018, **29**, 819–822.
- 51 R. Kitaura, G. Onoyama, H. Sakamoto, R. Matsuda, S. Noro and S. Kitagawa, *Angew. Chem., Int. Ed.*, 2004, **43**, 2684–2687.
- 52 B. Chen, X. Zhao, A. Putkham, K. Hong, E. B. Lobkovsky, E. J. Hurtado, A. J. Fletcher and K. M. Thomas, *J. Am. Chem. Soc.*, 2008, **130**, 6411–6423.
- 53 C. M. McGuirk, M. J. Katz, C. L. Stern, A. A. Sarjeant, J. T. Hupp, O. K. Farha and C. A. Mirkin, *J. Am. Chem. Soc.*, 2015, **137**, 919–925.
- 54 Z. F. Ju, S. C. Yan and D. Q. Yuan, *Chem. Mater.*, 2016, **28**, 2000–2010.
- 55 F. Song, C. Wang, J. M. Falkowski, L. Ma and W. Lin, *J. Am. Chem. Soc.*, 2010, **132**, 15390–15398.
- 56 S. H. Cho, B. Ma, S. T. Nguyen, J. T. Hupp and T. E. Albrecht-Schmitt, *Chem. Commun.*, 2006, 2563–2565.
- 57 S. C. Xiang, Z. Zhang, C. G. Zhao, K. Hong, X. Zhao, D. R. Ding, M. H. Xie, C. D. Wu, M. C. Das, R. Gill, K. M. Thomas and B. Chen, *Nat. Commun.*, 2011, **2**, 204.
- 58 Y. Cui, H. L. Ngo, P. S. White and W. Lin, *Chem. Commun.*, 2003, 994–995.
- 59 C. D. Wu, A. Hu, L. Zhang and W. Lin, *J. Am. Chem. Soc.*, 2005, **127**, 8940–8941.
- 60 S. Regati, Y. He, M. Thimmaiah, P. Li, S. Xiang, B. Chen and J. C. Zhao, *Chem. Commun.*, 2013, **49**, 9836–9838.
- 61 Z. Zhang, Y. R. Ji, L. Wojtas, W. Y. Gao, S. Ma, M. J. Zaworotko and J. C. Antilla, *Chem. Commun.*, 2013, **49**, 7693–7695.
- 62 M. Zheng, Y. Liu, C. Wang, S. Liu and W. Lin, *Chem. Sci.*, 2012, **3**, 2623.
- 63 W. Gong, X. Chen, H. Jiang, D. Chu, Y. Cui and Y. Liu, *J. Am. Chem. Soc.*, 2019, **141**, 7498–7508.
- 64 H. Y. An, E. B. Wang, D. R. Xiao, Y. G. Li, Z. M. Su and L. Xu, *Angew. Chem., Int. Ed.*, 2006, **45**, 904–908.
- 65 M. J. Ingleson, J. Bacsá and M. J. Rosseinsky, *Chem. Commun.*, 2007, 3036–3038.
- 66 Q. Ye, Y. M. Song, G. X. Wang, K. Chen, D. W. Fu, P. W. Chan, J. S. Zhu, S. D. Huang and R. G. Xiong, *J. Am. Chem. Soc.*, 2006, **128**, 6554–6555.
- 67 J. J. Qian, F. L. Jiang, D. Q. Yuan, X. J. Li, L. J. Zhang, K. Z. Su and M. C. Hong, *J. Mater. Chem. A*, 2013, **1**, 9075–9082.
- 68 J. Pang, F. Jiang, M. Wu, C. Liu, K. Su, W. Lu, D. Yuan and M. Hong, *Nat. Commun.*, 2015, **6**, 7575.
- 69 B. Li, W. Wang, Z. Hong, E. M. El-Sayed and D. Yuan, *Chem. Commun.*, 2019, **55**, 6926–6929.
- 70 S. S.-Y. Chui, S. M.-F. Lo, J. P. H. Charmant, A. G. Orpen and I. D. Williams, *Science*, 1999, **283**, 1148–1150.
- 71 Z. X. Xu, Y. X. Tan, H. R. Fu, J. Liu and J. Zhang, *Inorg. Chem.*, 2014, **53**, 12199–12204.
- 72 S.-Y. Zhang, C.-X. Yang, W. Shi, X.-P. Yan, P. Cheng, L. Wojtas and M. J. Zaworotko, *Chem*, 2017, **3**, 281–289.
- 73 Y. Liu, W. Xuan and Y. Cui, *Adv. Mater.*, 2010, **22**, 4112–4135.
- 74 Z. X. Xu, H. R. Fu, X. Wu, Y. Kang and J. Zhang, *Chem. – Eur. J.*, 2015, **21**, 10236–10240.
- 75 Z. X. Xu, Y. X. Tan, H. R. Fu, Y. Kang and J. Zhang, *Chem. Commun.*, 2015, **51**, 2565–2568.
- 76 C. Zhuo, Y. Wen, S. Hu, T. Sheng, R. Fu, Z. Xue, H. Zhang, H. Li, J. Yuan, X. Chen and X. Wu, *Inorg. Chem.*, 2017, **56**, 6275–6280.
- 77 D. Alezi, A. M. Peedikakkal, L. J. Weselinski, V. Guillermin, Y. Belmabkhout, A. J. Cairns, Z. Chen, L. Wojtas and M. Eddaoudi, *J. Am. Chem. Soc.*, 2015, **137**, 5421–5430.
- 78 S. Yuan, T. F. Liu, D. Feng, J. Tian, K. Wang, J. Qin, Q. Zhang, Y. P. Chen, M. Bosch, L. Zou, S. J. Teat, S. J. Dalgarno and H. C. Zhou, *Chem. Sci.*, 2015, **6**, 3926–3930.



- 79 G. Lan, K. Ni, S. S. Veroneau, X. Feng, G. T. Nash, T. Luo, Z. Xu and W. Lin, *J. Am. Chem. Soc.*, 2019, **141**, 4204–4208.
- 80 J. Castells-Gil, N. M. Padial, N. Almora-Barrios, J. Albero, A. R. Ruiz-Salvador, J. Gonzalez-Platas, H. Garcia and C. Marti-Gastaldo, *Angew. Chem., Int. Ed.*, 2018, **57**, 8453–8457.
- 81 M. H. Beyzavi, N. A. Vermeulen, A. J. Howarth, S. Tussupbayev, A. B. League, N. M. Schweitzer, J. R. Gallagher, A. E. Platero-Prats, N. Hafezi, A. A. Sarjeant, J. T. Miller, K. W. Chapman, J. F. Stoddart, C. J. Cramer, J. T. Hupp and O. K. Farha, *J. Am. Chem. Soc.*, 2015, **137**, 13624–13631.
- 82 L. Cao, Z. Lin, F. Peng, W. Wang, R. Huang, C. Wang, J. Yan, J. Liang, Z. Zhang, T. Zhang, L. Long, J. Sun and W. Lin, *Angew. Chem., Int. Ed.*, 2016, **55**, 4962–4966.
- 83 J. H. Cavka, S. Jakobsen, U. Olsbye, N. Guillou, C. Lamberti, S. Bordiga and K. P. Lillerud, *J. Am. Chem. Soc.*, 2008, **130**, 13850–13851.
- 84 A. Schaate, P. Roy, A. Godt, J. Lippke, F. Waltz, M. Wiebcke and P. Behrens, *Chem. – Eur. J.*, 2011, **17**, 6643–6651.
- 85 R. J. Marshall, C. L. Hobday, C. F. Murphie, S. L. Griffin, C. A. Morrison, S. A. Moggach and R. S. Forgan, *J. Mater. Chem. A*, 2016, **4**, 6955–6963.
- 86 Z. Lin, A. M. Slawin and R. E. Morris, *J. Am. Chem. Soc.*, 2007, **129**, 4880–4881.
- 87 D. Dang, P. Wu, C. He, Z. Xie and C. Duan, *J. Am. Chem. Soc.*, 2010, **132**, 14321–14323.
- 88 S. Y. Zhang, D. Li, D. Guo, H. Zhang, W. Shi, P. Cheng, L. Wojtas and M. J. Zaworotko, *J. Am. Chem. Soc.*, 2015, **137**, 15406–15409.
- 89 D. Yuan, D. Zhao, D. J. Timmons and H.-C. Zhou, *Chem. Sci.*, 2011, **2**, 103–106.
- 90 G. C. Shearer, S. Chavan, S. Bordiga, S. Svelle, U. Olsbye and K. P. Lillerud, *Chem. Mater.*, 2016, **28**, 3749–3761.
- 91 G. C. Shearer, J. G. Vitillo, S. Bordiga, S. Svelle, U. Olsbye and K. P. Lillerud, *Chem. Mater.*, 2016, **28**, 7190–7193.
- 92 B. Slater, Z. Wang, S. Jiang, M. R. Hill and B. P. Ladewig, *J. Am. Chem. Soc.*, 2017, **139**, 18322–18327.
- 93 J. Pang, S. Yuan, J. Qin, M. Wu, C. T. Lollar, J. Li, N. Huang, B. Li, P. Zhang and H. C. Zhou, *J. Am. Chem. Soc.*, 2018, **140**, 12328–12332.
- 94 H. Wang, X. Dong, J. Lin, S. J. Teat, S. Jensen, J. Cure, E. V. Alexandrov, Q. Xia, K. Tan, Q. Wang, D. H. Olson, D. M. Proserpio, Y. J. Chabal, T. Thonhauser, J. Sun, Y. Han and J. Li, *Nat. Commun.*, 2018, **9**, 1745.
- 95 S. Yuan, W. Lu, Y. P. Chen, Q. Zhang, T. F. Liu, D. Feng, X. Wang, J. Qin and H. C. Zhou, *J. Am. Chem. Soc.*, 2015, **137**, 3177–3180.
- 96 S. Yuan, Y. P. Chen, J. S. Qin, W. Lu, L. Zou, Q. Zhang, X. Wang, X. Sun and H. C. Zhou, *J. Am. Chem. Soc.*, 2016, **138**, 8912–8919.
- 97 C. X. Chen, Z. Wei, J. J. Jjiang, Y. Z. Fan, S. P. Zheng, C. C. Cao, Y. H. Li, D. Fenske and C. Y. Su, *Angew. Chem., Int. Ed.*, 2016, **55**, 9932–9936.
- 98 K. D. Nguyen, C. Kutzscher, F. Drache, I. Senkovska and S. Kaskel, *Inorg. Chem.*, 2018, **57**, 1483–1489.
- 99 X. Feng, H. S. Jena, K. Leus, G. Wang, J. Ouwehand and P. Van Der Voort, *J. Catal.*, 2018, **365**, 36–42.
- 100 Z.-X. Xu, Y. Liu and J. Zhang, *Inorg. Chem. Commun.*, 2016, **67**, 44–46.
- 101 G. Ferey, C. Mellot-Draznieks, C. Serre, F. Millange, J. Dutour, S. Surble and I. Margiolaki, *Science*, 2005, **309**, 2040–2042.
- 102 M. Banerjee, S. Das, M. Yoon, H. J. Choi, M. H. Hyun, S. M. Park, G. Seo and K. Kim, *J. Am. Chem. Soc.*, 2009, **131**, 7524–7525.
- 103 J. Chen, X. Chen, Z. Zhang, Z. Bao, H. Xing, Q. Yang and Q. Ren, *Mol. Catal.*, 2018, **445**, 163–169.
- 104 W. Zhu, C. He, P. Wu, X. Wu and C. Duan, *Dalton Trans.*, 2012, **41**, 3072–3077.
- 105 J. Canivet, S. Aguado, G. Bergeret and D. Farrusseng, *Chem. Commun.*, 2011, **47**, 11650–11652.
- 106 J. Bonnefoy, A. Legrand, E. A. Quadrelli, J. Canivet and D. Farrusseng, *J. Am. Chem. Soc.*, 2015, **137**, 9409–9416.
- 107 D. J. Lun, G. I. Waterhouse and S. G. Telfer, *J. Am. Chem. Soc.*, 2011, **133**, 5806–5809.
- 108 H. Furukawa, K. E. Cordova, M. O’Keeffe and O. M. Yaghi, *Science*, 2013, **341**, 1230444.
- 109 C. Kutzscher, H. C. Hoffmann, S. Krause, U. Stoeck, I. Senkovska, E. Brunner and S. Kaskel, *Inorg. Chem.*, 2015, **54**, 1003–1009.
- 110 S. Nießing, C. Czekelius and C. Janiak, *Catal. Commun.*, 2017, **95**, 12–15.
- 111 C. Kutzscher, G. Nickerl, I. Senkovska, V. Bon and S. Kaskel, *Chem. Mater.*, 2016, **28**, 2573–2580.
- 112 D. De, T. K. Pal and P. K. Bharadwaj, *Inorg. Chem.*, 2016, **55**, 6842–6844.
- 113 M. Sartor, T. Stein, F. Hoffmann and M. Fröba, *Chem. Mater.*, 2016, **28**, 519–528.
- 114 N. L. Rosi, J. Kim, M. Eddaoudi, B. Chen, M. O’Keeffe and O. M. Yaghi, *J. Am. Chem. Soc.*, 2005, **127**, 1504–1518.
- 115 H. Deng, S. Grunder, K. E. Cordova, C. Valente, H. Furukawa, M. Hmadeh, F. Gandara, A. C. Whalley, Z. Liu, S. Asahina, H. Kazumori, M. O’Keeffe, O. Terasaki, J. F. Stoddart and O. M. Yaghi, *Science*, 2012, **336**, 1018–1023.
- 116 D. J. Xiao, J. Oktawiec, P. J. Milner and J. R. Long, *J. Am. Chem. Soc.*, 2016, **138**, 14371–14379.
- 117 A. M. Fracaroli, P. Siman, D. A. Nagib, M. Suzuki, H. Furukawa, F. D. Toste and O. M. Yaghi, *J. Am. Chem. Soc.*, 2016, **138**, 8352–8355.
- 118 H. Deng, C. J. Doonan, H. Furukawa, R. B. Ferreira, J. Towne, C. B. Knobler, B. Wang and O. M. Yaghi, *Science*, 2010, **327**, 846–850.
- 119 H. Furukawa, N. Ko, Y. B. Go, N. Aratani, S. B. Choi, E. Choi, A. O. Yazaydin, R. Q. Snurr, M. O’Keeffe, J. Kim and O. M. Yaghi, *Science*, 2010, **329**, 424–428.
- 120 K. Koh, A. G. Wong-Foy and A. J. Matzger, *Angew. Chem., Int. Ed.*, 2008, **47**, 677–680.
- 121 K. Koh, A. G. Wong-Foy and A. J. Matzger, *J. Am. Chem. Soc.*, 2010, **132**, 15005–15010.

- 122 C. X. Chen, Z. W. Wei, J. J. Jiang, S. P. Zheng, H. P. Wang, Q. F. Qiu, C. C. Cao, D. Fenske and C. Y. Su, *J. Am. Chem. Soc.*, 2017, **139**, 6034–6037.
- 123 L. Liu, K. Konstas, M. R. Hill and S. G. Telfer, *J. Am. Chem. Soc.*, 2013, **135**, 17731–17734.
- 124 L. Liu, T. Y. Zhou and S. G. Telfer, *J. Am. Chem. Soc.*, 2017, **139**, 13936–13943.
- 125 T. Y. Zhou, B. Auer, S. J. Lee and S. G. Telfer, *J. Am. Chem. Soc.*, 2019, **141**, 1577–1582.
- 126 F. Song, C. Wang and W. Lin, *Chem. Commun.*, 2011, **47**, 8256–8258.
- 127 Q. Xia, Z. Li, C. Tan, Y. Liu, W. Gong and Y. Cui, *J. Am. Chem. Soc.*, 2017, **139**, 8259–8266.
- 128 P. Wu, C. He, J. Wang, X. Peng, X. Li, Y. An and C. Duan, *J. Am. Chem. Soc.*, 2012, **134**, 14991–14999.
- 129 Z. Xia, C. He, X. Wang and C. Duan, *Nat. Commun.*, 2017, **8**, 361.
- 130 C. Zou, Z. Zhang, X. Xu, Q. Gong, J. Li and C. D. Wu, *J. Am. Chem. Soc.*, 2012, **134**, 87–90.
- 131 Q. Han, C. He, M. Zhao, B. Qi, J. Niu and C. Duan, *J. Am. Chem. Soc.*, 2013, **135**, 10186–10189.
- 132 Q. Han, B. Qi, W. Ren, C. He, J. Niu and C. Duan, *Nat. Commun.*, 2015, **6**, 10007.
- 133 Q. Han, W. Li, S. Wang, J. He, W. Du and M. Li, *ChemCatChem*, 2017, **9**, 1801–1807.
- 134 O. K. Farha, A. M. Shultz, A. A. Sarjeant, S. T. Nguyen and J. T. Hupp, *J. Am. Chem. Soc.*, 2011, **133**, 5652–5655.
- 135 D. Feng, Z. Y. Gu, J. R. Li, H. L. Jiang, Z. Wei and H. C. Zhou, *Angew. Chem., Int. Ed.*, 2012, **51**, 10307–10310.
- 136 X. L. Yang, M. H. Xie, C. Zou, Y. He, B. Chen, M. O’Keeffe and C. D. Wu, *J. Am. Chem. Soc.*, 2012, **134**, 10638–10645.
- 137 W. Y. Gao, L. Wojtas and S. Ma, *Chem. Commun.*, 2014, **50**, 5316–5318.
- 138 W. L. He, M. Zhao and C. D. Wu, *Angew. Chem., Int. Ed.*, 2019, **58**, 168–172.
- 139 B. List, R. A. Lerner and C. F. Barbas III, *J. Am. Chem. Soc.*, 2000, **122**, 2395–2396.
- 140 Y. Liu, X. Xi, C. Ye, T. Gong, Z. Yang and Y. Cui, *Angew. Chem., Int. Ed.*, 2014, **53**, 13821–13825.
- 141 Y. Zhang, X. Feng, S. Yuan, J. Zhou and B. Wang, *Inorg. Chem. Front.*, 2016, **3**, 896–909.
- 142 T. Kitao, Y. Zhang, S. Kitagawa, B. Wang and T. Uemura, *Chem. Soc. Rev.*, 2017, **46**, 3108–3133.
- 143 B. Le Ouay, S. Kitagawa and T. Uemura, *J. Am. Chem. Soc.*, 2017, **139**, 7886–7892.
- 144 C. S. Liu, M. Chen, J. Y. Tian, L. Wang, M. Li, S. M. Fang, X. Wang, L. M. Zhou, Z. W. Wang and M. Du, *Chem. – Eur. J.*, 2017, **23**, 3885–3890.
- 145 L. Peng, S. Yang, S. Jawahery, S. M. Moosavi, A. J. Huckaba, M. Asgari, E. Oveisi, M. K. Nazeeruddin, B. Smit and W. L. Queen, *J. Am. Chem. Soc.*, 2019, **141**, 12397–12405.
- 146 X.-W. Dong, Y. Yang, J.-X. Che, J. Zuo, X.-H. Li, L. Gao, Y.-Z. Hu and X.-Y. Liu, *Green Chem.*, 2018, **20**, 4085–4093.
- 147 X. Han, Q. Xia, J. Huang, Y. Liu, C. Tan and Y. Cui, *J. Am. Chem. Soc.*, 2017, **139**, 8693–8697.
- 148 H. Li, X. Feng, P. Shao, J. Chen, C. Li, S. Jayakumar and Q. Yang, *J. Mater. Chem. A*, 2019, **7**, 5482–5492.
- 149 L. H. Li, X. L. Feng, X. H. Cui, Y. X. Ma, S. Y. Ding and W. Wang, *J. Am. Chem. Soc.*, 2017, **139**, 6042–6045.
- 150 S. Yan, X. Guan, H. Li, D. Li, M. Xue, Y. Yan, V. Valtchev, S. Qiu and Q. Fang, *J. Am. Chem. Soc.*, 2019, **141**, 2920–2924.
- 151 X. Wu, X. Han, Q. Xu, Y. Liu, C. Yuan, S. Yang, Y. Liu, J. Jiang and Y. Cui, *J. Am. Chem. Soc.*, 2019, **141**, 7081–7089.
- 152 X. Wang, X. Han, J. Zhang, X. Wu, Y. Liu and Y. Cui, *J. Am. Chem. Soc.*, 2016, **138**, 12332–12335.
- 153 X. Han, J. Huang, C. Yuan, Y. Liu and Y. Cui, *J. Am. Chem. Soc.*, 2018, **140**, 892–895.
- 154 H. L. Qian, C. X. Yang and X. P. Yan, *Nat. Commun.*, 2016, **7**, 12104.
- 155 H. C. Ma, C. C. Zhao, G. J. Chen and Y. B. Dong, *Nat. Commun.*, 2019, **10**, 3368.
- 156 H. Xu, X. Chen, J. Gao, J. Lin, M. Addicoat, S. Irle and D. Jiang, *Chem. Commun.*, 2014, **50**, 1292–1294.
- 157 H. Xu, J. Gao and D. Jiang, *Nat. Chem.*, 2015, **7**, 905–912.
- 158 H. S. Xu, S. Y. Ding, W. K. An, H. Wu and W. Wang, *J. Am. Chem. Soc.*, 2016, **138**, 11489–11492.
- 159 J. Zhang, X. Han, X. Wu, Y. Liu and Y. Cui, *J. Am. Chem. Soc.*, 2017, **139**, 8277–8285.
- 160 J. Zhang, X. Han, X. Wu, Y. Liu and Y. Cui, *ACS Sustainable Chem. Eng.*, 2019, **7**, 5065–5071.
- 161 G. Liu, J. Sheng and Y. Zhao, *Sci. China Mater.*, 2017, **60**, 1015–1022.
- 162 S. Kandambeth, A. Mallick, B. Lukose, M. V. Mane, T. Heine and R. Banerjee, *J. Am. Chem. Soc.*, 2012, **134**, 19524–19527.
- 163 M. J. Ingleson, J. P. Barrio, J. Bacsá, C. Dickinson, H. Park and M. J. Rosseinsky, *Chem. Commun.*, 2008, 1287–1289.
- 164 S. Lee, E. A. Kapustin and O. M. Yaghi, *Science*, 2016, **353**, 808–811.
- 165 Y. Inokuma, S. Yoshioka, J. Ariyoshi, T. Arai, Y. Hitora, K. Takada, S. Matsunaga, K. Rissanen and M. Fujita, *Nature*, 2013, **495**, 461–466.